

NUMERICAL ASPECTS AND SOURCE TERM ANALYSIS OF WAVE MODELING IN A TIDAL INLET

Gerbrant van Vledder^{1,3}, Jacco Groeneweg², André van der Westhuysen²
and Ap van Dongeren².

¹Alkyon Hydraulic Consultancy & Research, P.O. Box 248, 8300AE Emmeloord,
The Netherlands

²WL|Delft Hydraulics, PO Box 177, 2600 MH, Delft, The Netherlands

³Delft University of Technology, P.O. Box 5048, 2600 GA, Delft, The Netherlands

INTRODUCTION

Dikes protect large parts of the Netherlands against storm surges and wave attack. As described in Van Dongeren et al. (2007), these primary coastal defenses must be checked every five years by the best available methods to verify whether they comply with the required level of protection on the basis of Hydraulic Boundary Conditions (HBC). For a location along a primary coastal defense the HBC consist of a combination of normative wave conditions and water levels. Presently, a number of model studies are carried out in the framework of the SBW (*Sterkte en Belasting Waterkeringen: Strength and Loads on Water Defenses*) with the overall aim to improve the quality of the models and methods used to derive these HBC in the Wadden Sea. This is a shallow sea in the north of the Netherlands and protected from the North Sea by a number of barrier islands (Figure 1). Tidal flows enter and leave the Wadden Sea via a number of tidal inlets. North Sea waves may also penetrate through these tidal inlets in the Wadden Sea and contribute to the wave loads on the dikes of the Wadden Sea in addition to locally generated waves.

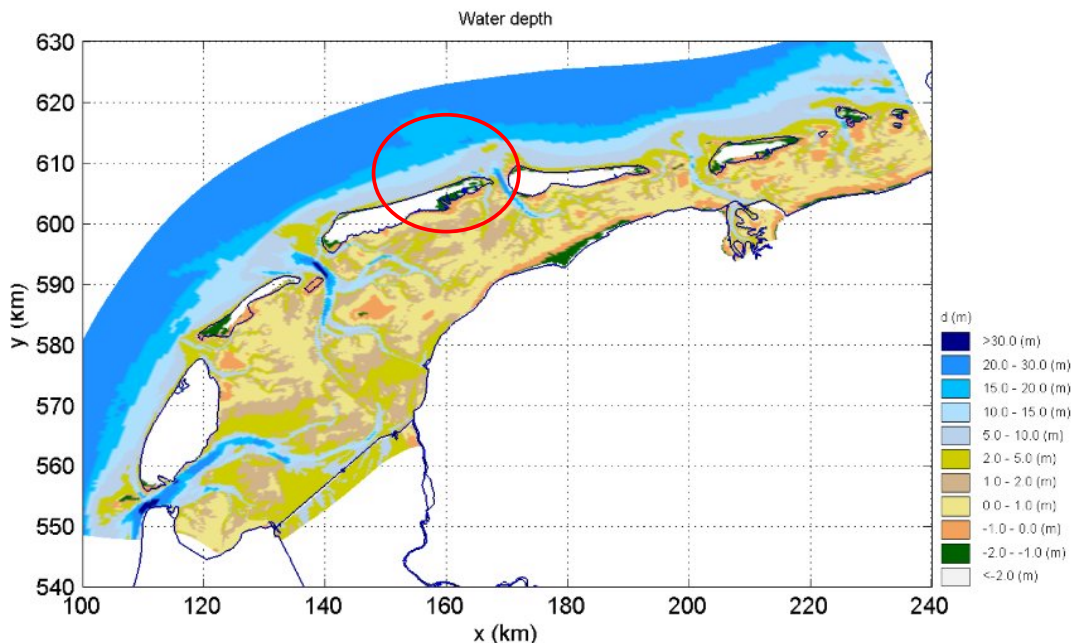


Figure 1: Bathymetry of the Wadden Sea based on depth soundings from 1999 (encircled: tidal inlet of Ameland)

In view of its geometry, it is expected that the wave conditions in the Wadden Sea are determined by local wave growth, depth limitations and swell waves that penetrate through the tidal inlets. In addition, tidal flows will affect the waves in the tidal inlets. The modeling of waves in such conditions is not straightforward since they are affected by many different processes. Therefore, one of the studies conducted within the SBW framework is to determine the best modelling approach using the SWAN model (Booij et al. 1999) to compute storm waves in a tidal inlet. In this paper the focus is on the tidal inlet of Ameland (encircled in Figure 1). It is noted that in the SWAN computations presented in this paper a depth schematisation based on depth soundings from the years 2004 to 2006 was used.

The paper consists of two parts of the larger study. The first part addresses the requirements with respect to the computational grids and convergence behaviour of SWAN. The second part focuses on the role of the physical processes in the tidal inlet whether North Sea storm waves penetrate into the Wadden Sea. A good understanding of these processes is important for the further development and application of these models. Both parts are important for applying the SWAN model for the determination of the HBC. Efficiency is relevant since hundreds of computations need to be carried out, and accurate results are important for the quality of the HBC.

OPTIMIZATION OF COMPUTATIONAL GRIDS

In The Netherlands, the SWAN model is often used in combination with the WAQUA flow model, which provides current and water level fields. Since the WAQUA model uses non-uniform grids it is common practice to use the same computational grid to minimize interpolation errors. This choice, however, does not always lead to optimal computational grids from the viewpoint of wave modelling. This is because the choice of the grid resolution is determined by the spatial variation of the variables to be solved. The water levels and currents, computed by WAQUA, typically show variability in areas that are different from the areas where the wave action density strongly varies. For instance, in the surf zone wave conditions show stronger variations than currents. Furthermore, the numerical scheme of the WAQUA flow model requires that the curvi-linear grid is close to orthogonal and that the variation of grid cell sizes varies gradually. These requirements are less strict for the numerical propagation schemes used in most wave models. The reason it that wave model use hyperbolic propagation schemes without diffusion terms, whereas flow models (at least WAQUA) use parabolic propagation schemes including diffusion terms.

A criterion for the optimization of wave model grids is a sufficiently fine resolution in areas with large gradients in wave conditions due to variations in either current speed or bathymetry. Following this line of reasoning numerical tests were carried out with SWAN in 1D mode to find the optimal resolution for wave propagation in an area with a large variation in wave conditions. To that end a simple 1D geometry was set up, including a steep slope where the incident deep water waves become depth-limited. Using the normalized gradients of the computed significant wave height H_{m0} and spectral period $T_{m-1,0}$ relations were derived to couple the required spatial resolution to the gradients in these wave parameters according to

$$\Delta x \propto \frac{\mu_H}{|\nabla H_{m0}| / |H_{m0}|} \tag{1}$$

$$\Delta x \propto \frac{\mu_H}{|\nabla T_{m-1,0}| / |T_{m-1,0}|}$$

where ∇ is the horizontal gradient operator. Based on the SWAN 1D computations the proportionally coefficients were estimated as $\mu_H \approx 200$ and $\mu_T \approx 150$, with Δx in m, H_{m0} in m and $T_{m-1,0}$ in s.

These guidelines were applied to make a dedicated non-uniform wave model grid for the tidal inlet of Ameland. To that end, a severe storm situation was simulated using a fine regular grid enveloping this tidal inlet and part of the Wadden Sea to find the required gradient. Subsequently, the normalized gradients in the significant wave height H_{m0} and spectral wave period $T_{m-1,0}$ were determined. The spatial variations of these gradients are shown in the Figures 2 and 3 together with the 5 m, 10 m and 20 m depth contours. As expected the largest gradients occur in the shallow areas on the edge of the ebb tidal delta and along the nearshore zone of the Wadden islands. For the spectral period, narrow strips with large gradients are possibly related to refraction effects at the edges of the tidal channels.

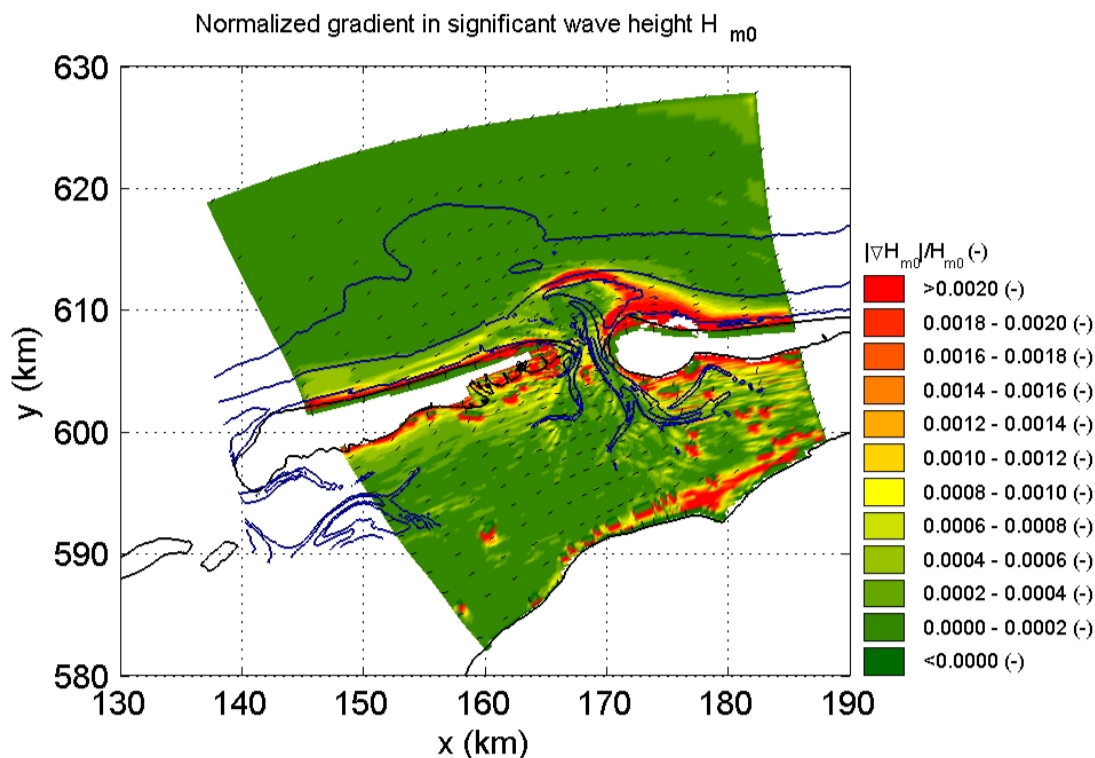


Figure 2: Normalized gradient of the significant wave height H_{m0} computed with SWAN for the tidal inlet of Ameland for the storm of 8 February 2004, 22:30 hours. Wind speed and direction were 15 m/s and 326° , the water level was NAP +2.54 m. Depth contours at NAP -5m, -10m and -20m.

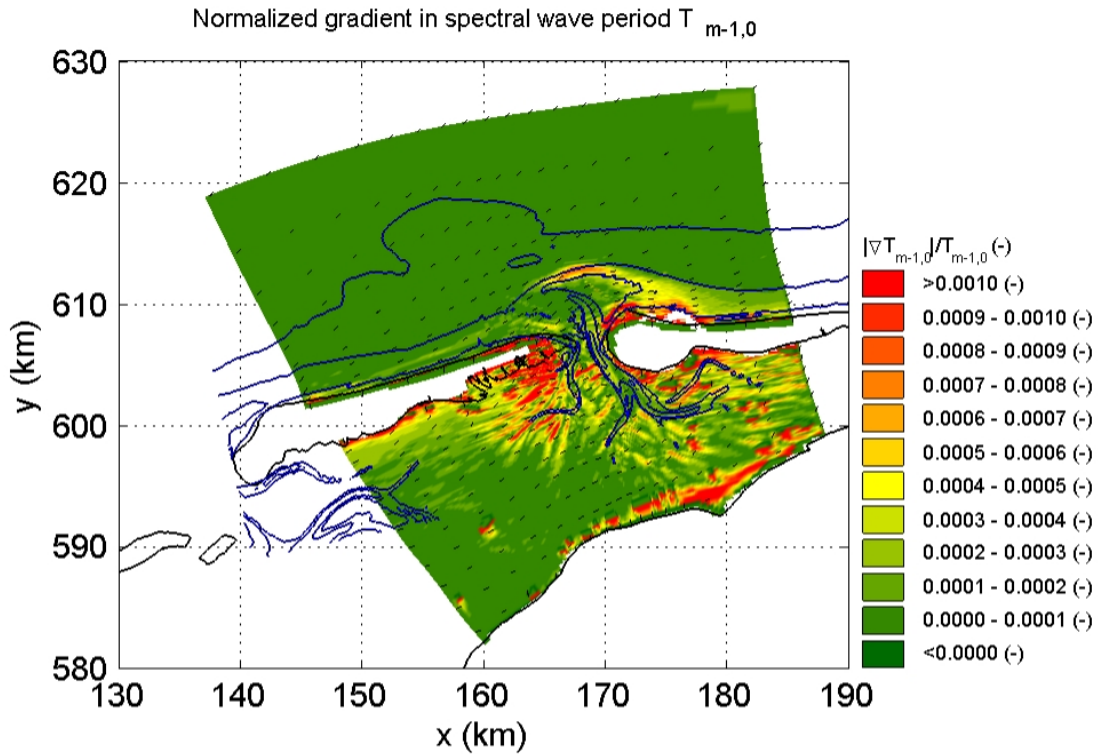


Figure 3: Normalized gradient of the spectral period $T_{m-1,0}$ computed with SWAN for the tidal inlet of Ameland for the storm of 8 February 2004, 22:30 hours. Wind speed and direction were 15 m/s and 326° , the water level was NAP +2.54 m. Depth contours at NAP -5m, -10m and -20m.

The existing non-uniform grid used in the WAQUA model simulations was used as a basis for constructing a dedicated non-uniform grid for SWAN. A section of this WAQUA grid is shown in the upper panel of Figure 4. For clarity only every second grid line is shown. This grid is only slightly curved and the spatial variation in cell size is small. Thus, it can be considered as a quasi-rectangular grid. The next step was to apply the rules for the grid spacing on the basis of the computed gradients in wave parameters. As can be seen in the Figures 2 and 3 large gradients in both parameters appear in the central and shallow part of the tidal inlet. Especially large gradients occur on the outer edge of the ebb-tidal delta. Using this information a method was developed to shift the grid points of the original grid to obtain a finer resolution in the tidal inlet. At the same time an overall increase in resolution was achieved by adding additional (2, 3 or 4) grid points along the sides of each grid cell. For instance, a doubling of the number of grid points in both directions then results in four-fold number of grid points. To avoid too much spatial variation in cell size, an omni-directional approach was followed such that the finest resolution occurs in the central part of the tidal inlet, with increasing cell sizes extending outward in all directions. Various tests were carried out to determine which resolution produces, using the least number of grid points, results that are the closest to those of a rectangular grid with a very fine resolution. Optimal results were obtained with an increase of the spatial resolution with a factor 3 in both directions and a refinement of the resolution in the central part of tidal inlet. The result of this optimization is shown in the lower panel of Figure 4 (for clarity every sixth grid line is shown).

The resolution in the central part of the tidal inlet is about 50 m, near the dikes of the mainland the resolution decreased to about 150 m. The dedicated non-uniform grid uses 60% less grid points and CPU time than an equally fine (in the central part of the tidal inlet) WAQUA grid obtained by increasing the resolution in both directions with a factor 4. Details of this optimization can be found in Alkyon, DUT, NRL and WL (2007).

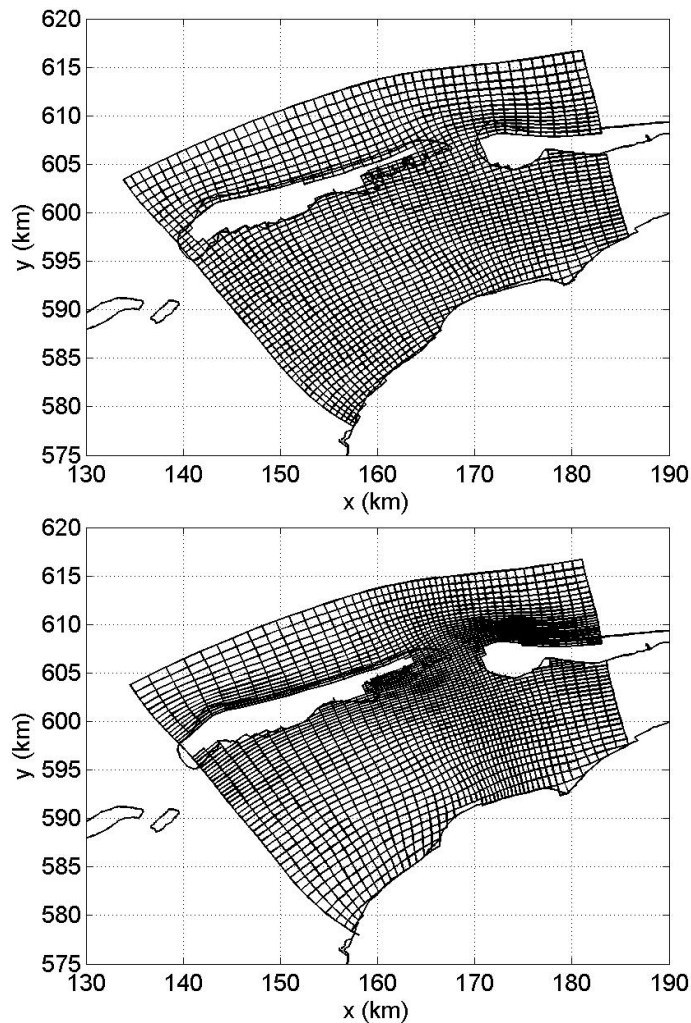


Figure 4: Outlines of original (WAQUA) curvi-linear grid for the Wadden Sea (upper panel) and the dedicated non-uniform grid for the tidal inlet of Ameland (lower panel). For clarity every second line is shown in the upper panel and every sixth line in the lower panel.

CONVERGENCE BEHAVIOUR

The SWAN model uses an iterative procedure to solve the action balance equation. The number of required iterations is prescribed by so-called convergence criteria. The present SWAN version (40.51) uses the curvature criterion developed by Zijlema and Van der Westhuysen (2005). This criterion uses the second derivative of the changes in the significant wave height between three successive iterations. The iteration stops when the curvature is less than a certain threshold in, say, 99.5% of all grid points. A limitation of this convergence criterion is that, since it is based on

only the significant wave height, it is not guaranteed that converged results are obtained for other integral parameters, such as the spectral period $T_{m-1,0}$, the mean direction θ and the directional spreading σ . Moreover, the user does not obtain information about the locations where the convergence criterion is not met.

Detailed information on the convergence behaviour of SWAN was obtained by inspection of the change in the significant wave height between two iterations during various phases in the iteration process. In addition, the development of the 2D-spectrum and related spectral parameters were analysed in a number of points of the computational grid. An example of the change in significant wave height after 15 iterations is shown in Figure 5. This figure clearly shows that the convergence behaviour is not uniformly distributed in space. Insignificant changes occur in large areas of the computational grid, whereas relatively large changes still occur in some well-defined areas. The implication of this finding is that even more iterations are needed to obtain the required convergence in all areas.

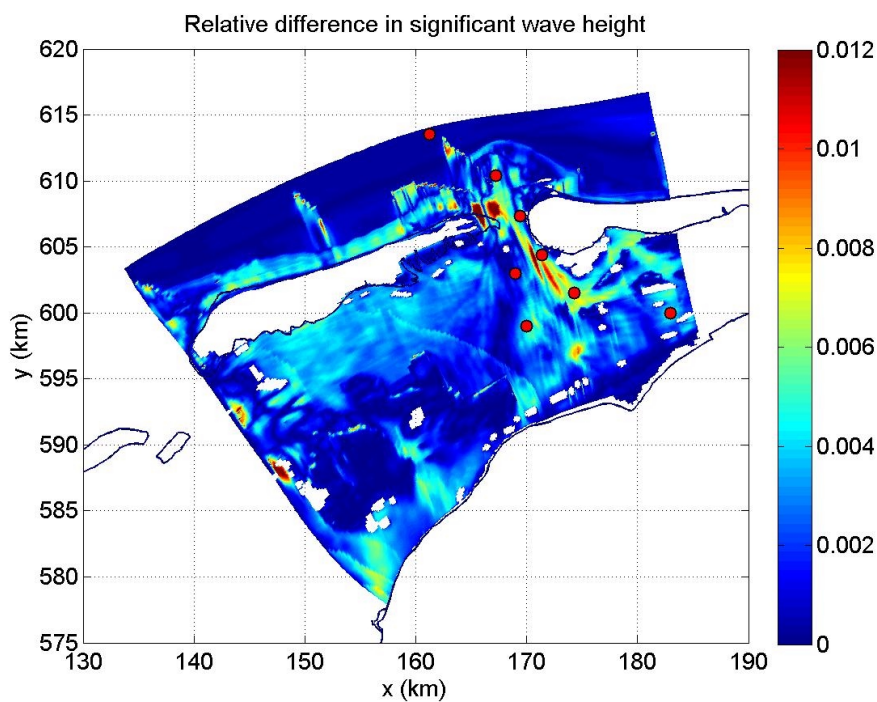


Figure 5: Change in significant wave height in m after 15 iterations. Computed with SWAN for the storm of 8 February 2004, 22:30 hours. Red points indicate output locations.

Figure 6 shows the convergence behaviour of the significant wave height H_{m0} , the spectral period T_{m-10} , the mean direction θ and the directional spreading σ integral parameters in a number of points, which are also shown in Figure 5. The convergence behaviour is highlighted in red and blue for two output points. These locations coincide with the areas with good and with poor convergence. Still, at some locations, no convergence is obtained after 100 iterations. The parameter values of all parameters, except the mean direction, are normalized with the corresponding value after 100 iterations.

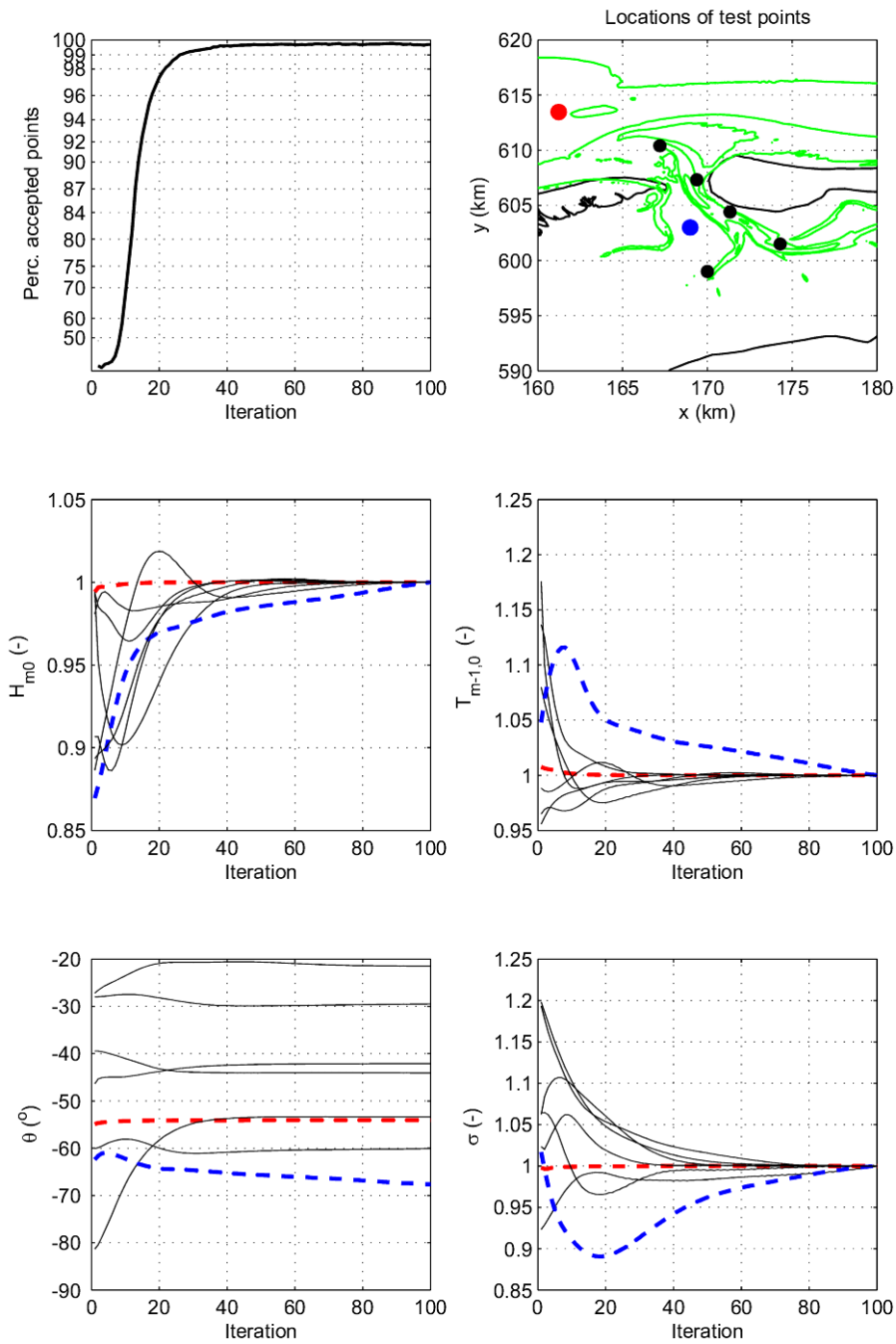


Figure 6: Convergence behaviour of the significant wave height H_{m0} , spectral period $T_{m-1,0}$, mean wave direction θ and directional spreading σ for a number of points in the tidal inlet of Ameland for the storm of 8 February 2004, 22:20 hours. The overall convergence behaviour is shown in the upper left panel. Output locations are shown in the upper right panel. Two locations and their convergence behaviour, given in red and blue, are highlighted.

The overall convergence behaviour is shown in the upper left panel. It is noted that with a 99.5% criterion convergence would be reached already after 32 iterations. The results clearly show that the convergence behaviour of the significant wave height H_{m0} , spectral period $T_{m-1,0}$ and mean wave direction are comparable, whereas the convergence behaviour of the directional spreading is poor. Still, at one test point the convergence is poor for all parameters.

The different rates of convergence of the spectral parameters suggest that the convergence criterion should be extended with the convergence behaviour of additional parameters, such as a spectral period or directional measures. In fact WL|Delft Hydraulics (2007) made a version of SWAN which includes the spectral period T_{m01} in the curvature criterion. A practical way to achieve a sufficient level of convergence is to first identify the areas with poor convergence, and secondly to create test output in these points showing the convergence behaviour of all relevant parameters. It is noted that the present SWAN version has the necessary output options to track the convergence behaviour in detail.

We note that the spatial variation of the convergence behaviour led to the development of a technique to speed up the convergence behaviour of SWAN in which grid points with more or less converged results were temporarily deactivated in the iteration process. Savings in CPU up to 40% were achieved. Details of this new technique can be found in WL | Delft Hydraulics (2007).

SOURCE TERM ANALYSIS

An important aspect of improving any wave model is to identify the origin of prediction errors. For the Wadden Sea situation, this was achieved by performing hindcast studies of storms in the tidal inlet of Ameland followed by a detailed analysis of the results. Important aspects of such an analysis are to compare the measured and computed wave spectra, and a statistical analysis of integral wave parameters. Examples thereof are described in Van Dongeren et al. (2007) and Alkyon (2007a, b).

Another approach is to analyse the spatial distribution of the magnitude of the physical processes as modelled in SWAN (see also Alkyon, 2007a, b). Using the HOTFILE output file option of SWAN, combined with depth and wind information, all source terms were reconstructed and their magnitude determined according to

$$M = \iint |S(f, \theta)| df d\theta \quad (2)$$

This technique was applied to the SWAN hindcast results of the storm of 17 December 2005. Most default settings of SWAN 40.51 were used for the activation of the physical processes. (SWAN team 2007), except for the whitecapping, which was evaluated using the saturation-based whitecapping of Van der Westhuysen et al. (2007).

Figure 7 shows the spatial variation of the magnitude of the source terms for wind input, whitecapping dissipation, and quadruplet interactions. The spatial variation of the shallow water source terms for surf breaking, bottom friction and triad interaction are shown in Figure 8. Since the magnitudes show differences up to a few orders of magnitude, they are plotted on log scale. The 5 m, 10 m and 20 m depth contours are shown as blue lines.

Figure 7 shows that wind input and whitecapping have similar magnitudes in most areas. They are weaker in the Wadden Sea than in the North Sea. The quadruplet interactions have similar magnitudes as the wind input and whitecapping, except on the edge of the ebb tidal delta where they become much stronger due to shallow water effects. Figure 8 shows that in the North Sea bottom friction has more or less the same magnitude as the deep water source terms. In the Wadden Sea and in the tidal channels in the inlet bottom friction becomes much weaker. Triad interactions and surf breaking are very strong in the shallow parts of the tidal inlet and in the shallow nearshore areas of the Wadden islands. The pattern of the magnitude of these two source terms reflects the bottom topography of the tidal inlet. In the Wadden Sea interior, the strength of these source terms is very weak.

Figure 9 presents the variation of the source term magnitude along the main output transect through the tidal inlet (see Figures 7 and 8). This allows a more quantitative comparison of the source term magnitudes. The source term investigations showed that depth-limited wave breaking and triad interactions are dominant in the shallow areas of the tidal inlet, whereas the ‘deep water’ source terms dominate in the Wadden Sea interior, where the depth limitation is less. It also implies that the tidal inlet acts as a strong filter for North Sea waves and that the wave conditions in the Wadden Sea seem to be determined by local wind sea growth.

To further analyse the physics (as modelled by SWAN), the spatial variation of some non-dimensional parameters was investigated. Figures 10 and 11 show the spatial variation of the dimensionless water depth kh (with k the mean wave number and h the water depth) and the mean wave steepness $s=H_m/L$ (with L the mean wave length), respectively. Figure 10 shows that very low values of kh (down to 0.5) are found along the edge of the ebb tidal delta. In this region, the quadruplet interaction expression used in SWAN is applied beyond its range of validity. The computed variation of the mean wave steepness shows unrealistically high values (up to 12%) just downwind of the Wadden islands, whereas in nature values up to 7% to 8% are found. This is a strong indication that initial wave growth is not properly modelled in the present version of the SWAN model.

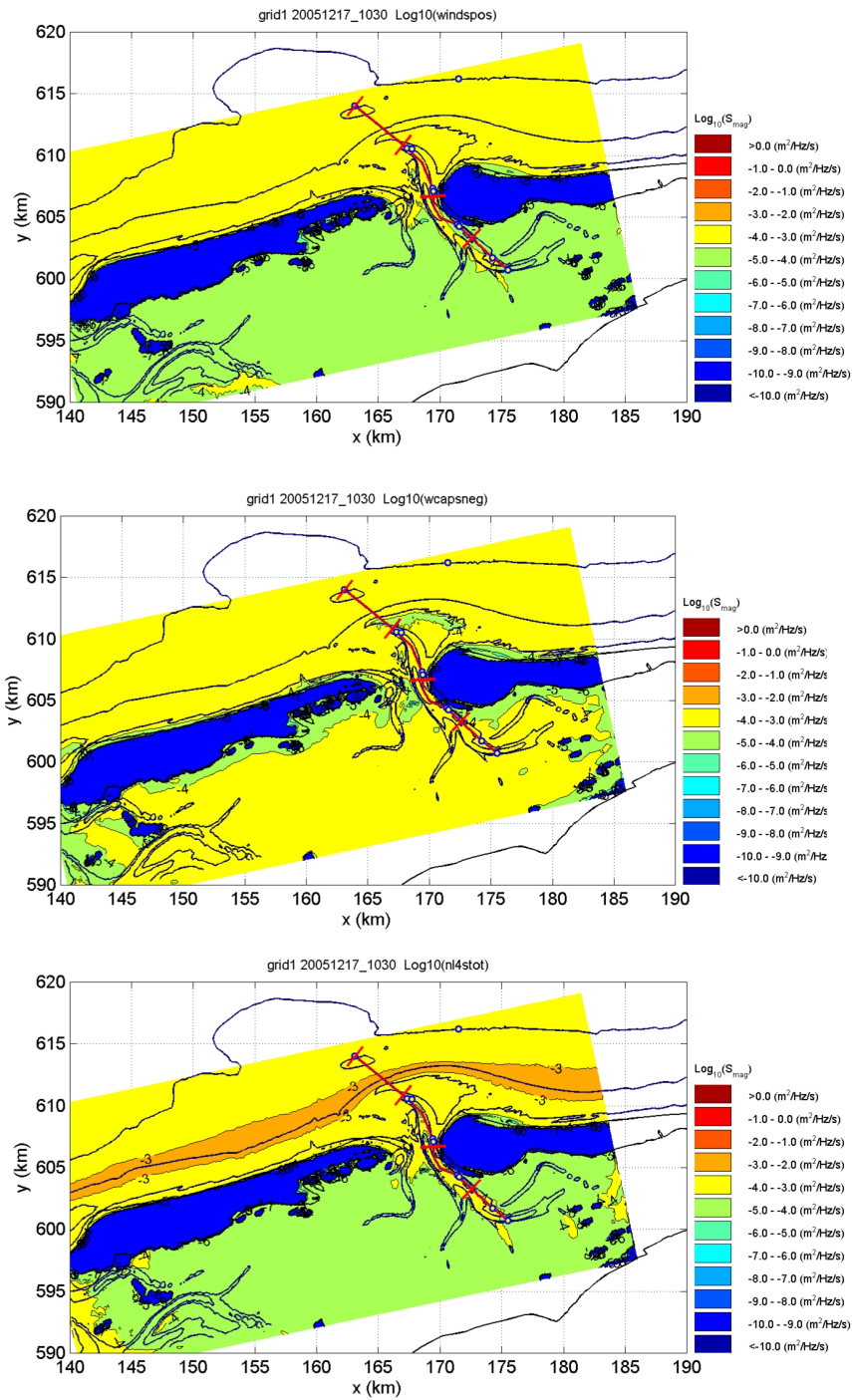


Figure 7: Spatial variation of the deep water source term magnitudes for wind input, whitecapping dissipation and quadruplets in the tidal inlet of Ameland for the storm of 17 December 2005, 10:30 hours. Wind speed and direction were 15.4 m/s and 329°, the water level was NAP +2.0 m.

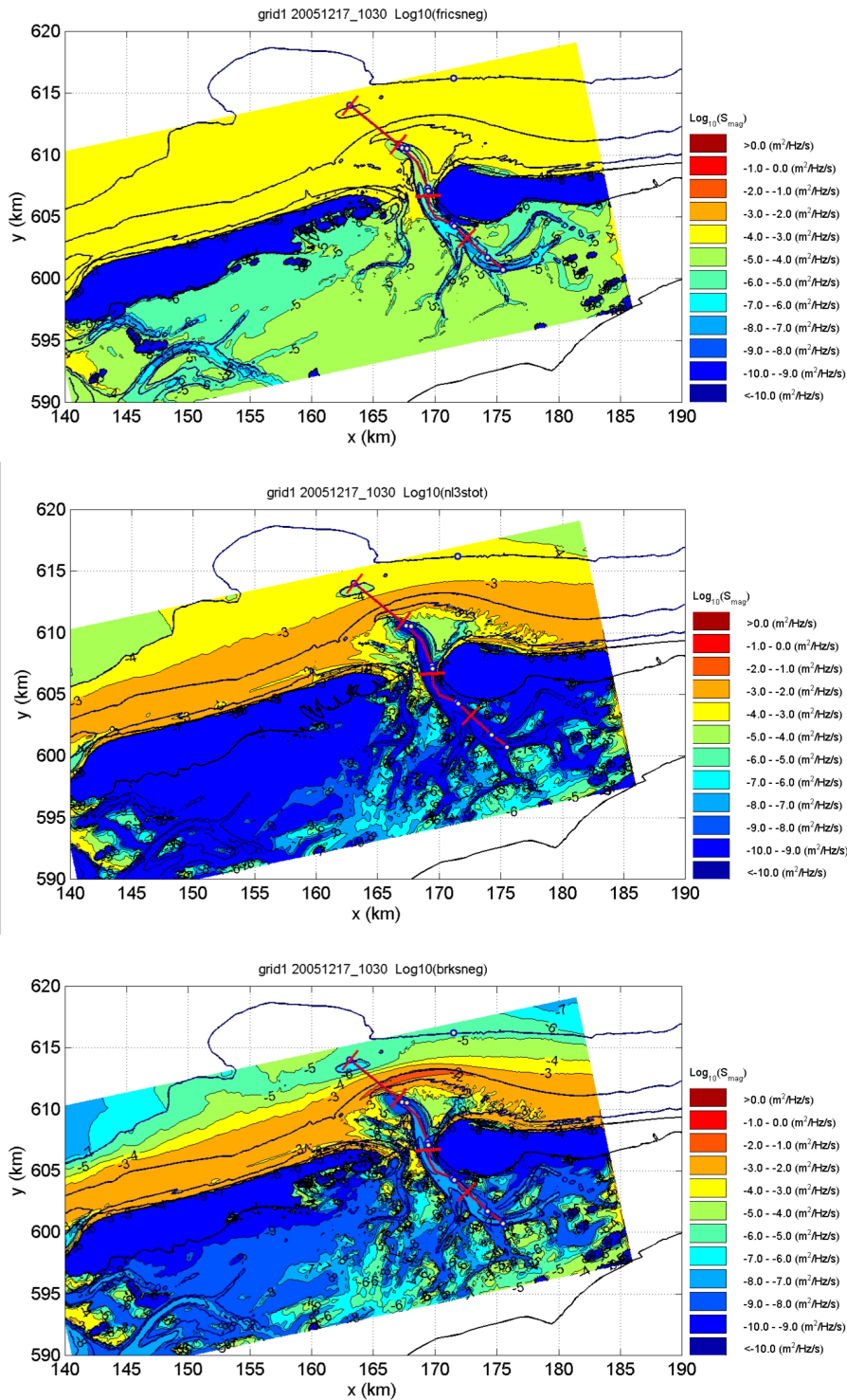


Figure 8: Spatial variation of the shallow water source term magnitudes for surf breaking, triad interactions and bottom friction in the tidal inlet of Ameland for the storm of 17 December 2005, 10:30 hours. Wind speed and direction were 15.4 m/s and 329°, the water level was NAP +2.0 m.

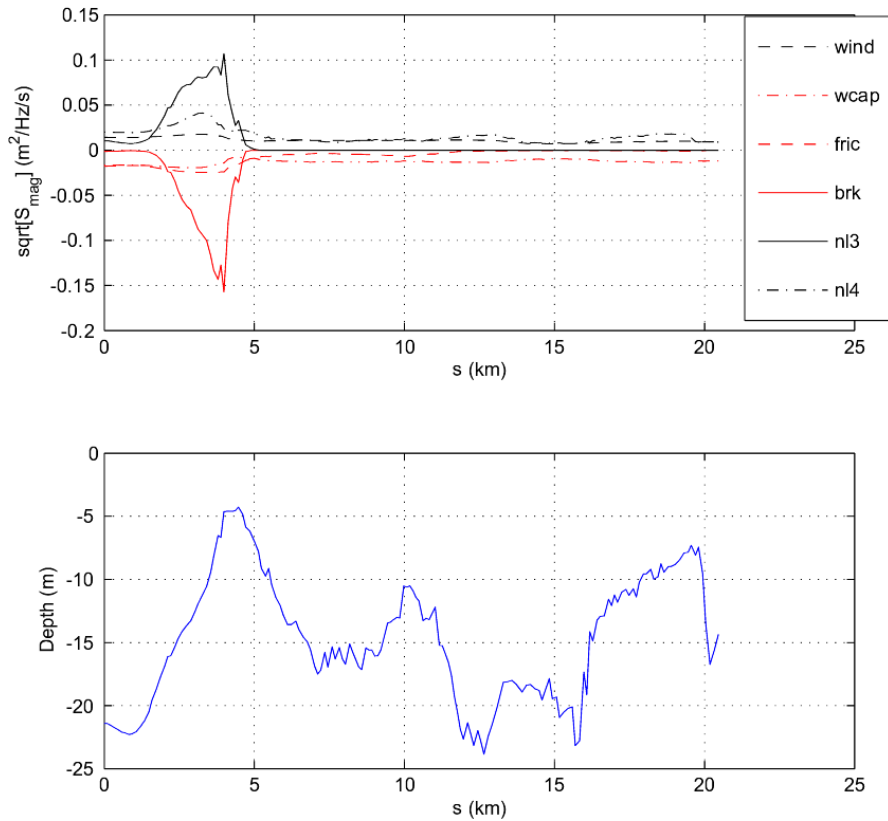


Figure 9: Variation of source term magnitude along the ray through the main tidal channel in the tidal inlet of Ameland. Based on the SWAN computations for the storm of 17 December 2005.

SWELL PENETRATION INTO THE WADDEN SEA

Of special interest is the propagation of swell waves through the tidal inlet. The occurrence of swell waves can be detected by inspection of the frequency spectra. As described in Van Dongeren (2007) such low frequency waves were not detected at the buoys located in the tidal channel just west of Ameland. Therefore, an indirect way to detect the amount of swell wave penetration was to compute the spatial variation of the ratios of the significant wave height H_{10} to the H_{m0} , and of the spectral periods T_{m01} and $T_{m-1,0}$. The parameter H_{10} is the significant wave height based on all wave components with periods longer than 10 s. Figure 12 shows the spatial variation of these ratios in the tidal inlet of Ameland for the storm of 17 December 2005. In the tidal inlet areas a relatively large amount of long period waves are visible by the green tongues that extend in the western part of the inlet. In most areas on the North Sea and in the Wadden Sea the wave period ratio is about 0.9 which points to a kind of equilibrium. Areas with a relative surplus of long period swell waves are identified by smaller values of this ratio. It can clearly be seen that these areas are located west of the main tidal channel on the shallow banks. This behaviour can be explained by the fact that the longer waves refract out of the channels and turn towards the shallower parts of the tidal inlet where they dissipate by wave breaking.

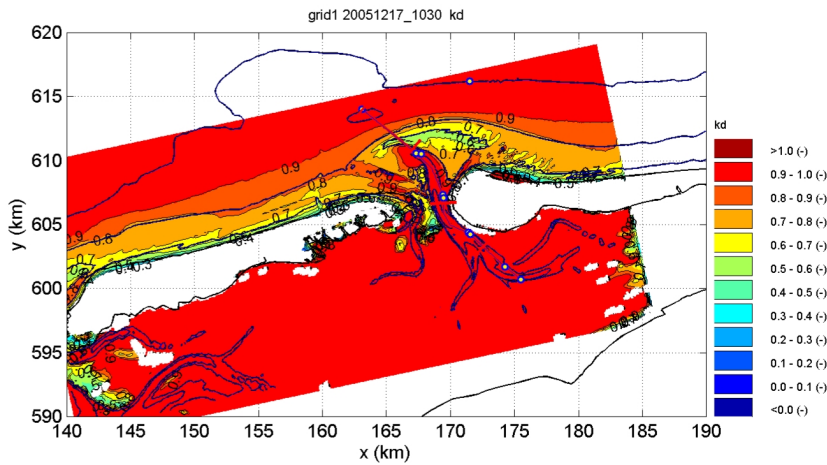


Figure 10: Spatial variation of the dimensionless water depth kh in the tidal inlet of Ameland for the storm of 17 December 2005, 10:30 hours.

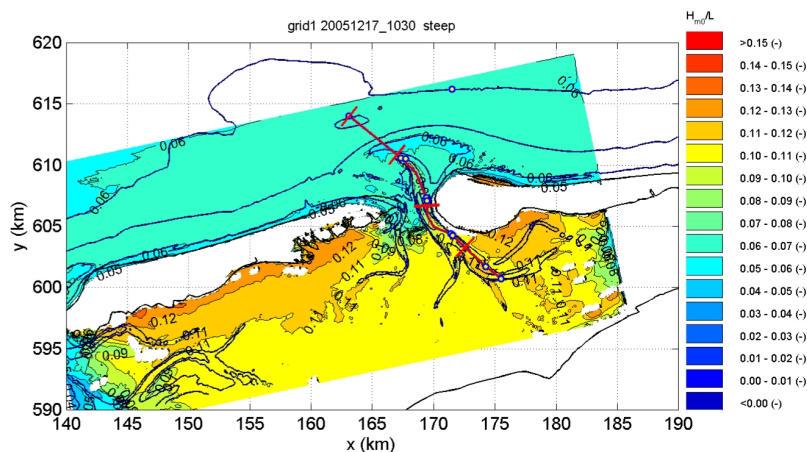


Figure 11: Spatial variation of mean wave steepness $s = H_{m0}/L$ in the tidal inlet of Ameland for the storm of 17 December 2005, 10:30 hours.

SUMMARY AND CONCLUSIONS

The present study has highlighted a number of possibilities to improve the numerics of SWAN and it pointed to a number of weak points in the modelling of the physical processes. Significant savings in computational requirements can be obtained by the construction of dedicated non-uniform grids for wave modelling in the Wadden Sea. The analysis of the convergence behaviour of SWAN has shown that the speed of convergence is not spatially uniform and that more iterations are needed to obtain the required convergence in all grid points than with the present criterion. In addition, it was found that the rate of convergence is slower for the directional spreading, which may also lead to more iterations than can be judged on the basis of the present wave height-based curvature criterion. However, the non-uniform spatial behaviour of the iteration processes was used to our advantage to develop a dynamic deactivation method to focus the computational work on those areas where more iterations are needed to obtain a converged solution.

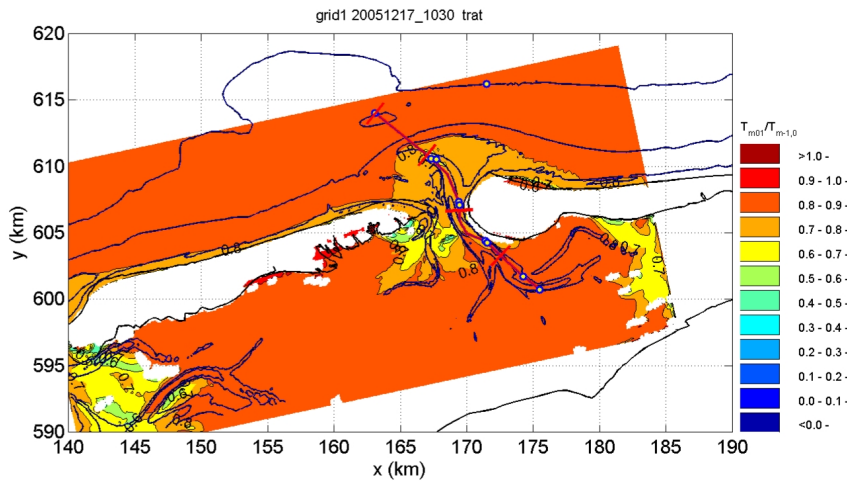
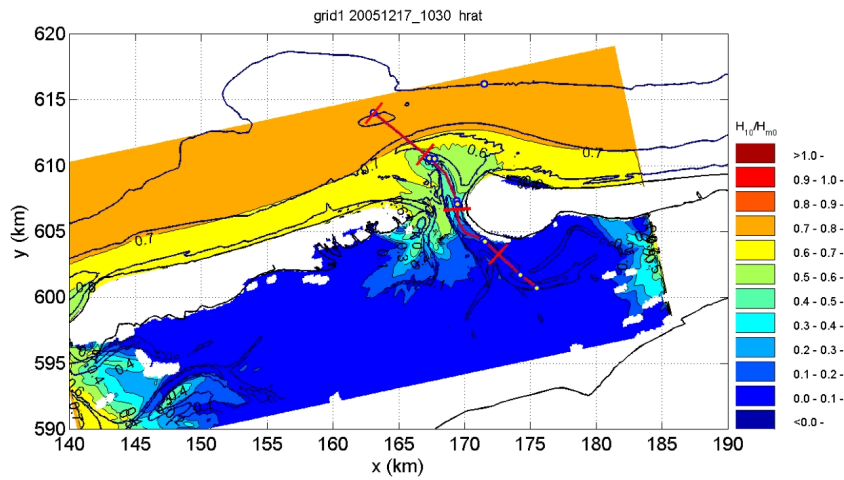


Figure 12: Spatial variation of the ratio of the wave height H_{10} and H_{m0} (upper panel) and the spectral periods T_{m01} and $T_{m-1,0}$ (lower panel) in the tidal inlet of Ameland for the storm of 17 December 2005, 10:30 hours.

The analysis of the source term magnitudes has shown that a lot of physical activity takes places in the shallow parts of the tidal inlet, where surf breaking and triad interaction dominate. Especially the surf breaking process is responsible for the strong reduction of North Sea waves. The analysis also showed that local (deep) water processes dominate in the Wadden Sea, at least for these storm conditions. It should be noted that these findings are based on (SWAN) model computations and verification against measurements is required. Further investigations are envisioned to analyses the source term balance under normative (super) storm conditions.

The analysis of the non-dimensional parameters showed that, in some areas, some source terms in SWAN (e.g. quadruplet interactions) are applied outside its assumed range of applicability. This also holds for the triads as based on the spatial distribution of the Ursell number (not shown). This

knowledge can be used to perform dedicated field or laboratory experiments aimed at improving the shallow water source terms in areas where strong physical effects occur. The same applies for initial wave growth at short fetches, where SWAN seems to overestimate the wave steepness.

The analysis of the swell penetration has shown that the relatively long swell waves refract out of the channels such that they appear on the shallow areas where they dissipate by wave breaking.

ACKNOWLEDGEMENTS

This study has been funded by the Ministry of Transport and Public Works in the Netherlands under contracts RKZ-1697 and RIKZ-1797.

REFERENCES

- Alkyon, 2007a, Analysis SWAN hindcast tidal inlet of Ameland, Storms of 8 February and 2, 8 January 2005. Alkyon report A1725r4. Author: G.Ph. van Vledder.
- Alkyon, 2007b, Analysis SWAN hindcast tidal inlet of Ameland, Storms of 17 December 2005 and 9 February 2006. Alkyon report A1725r5. Author: G.Ph. van Vledder.
- Alkyon, Delft University of Technology, Naval Research Laboratory and WL|Delft Hydraulics, 2007: Sensitivity analysis of numerical aspects of SWAN. Report H4803.60/A1725R5. Authors: G.Ph. van Vledder, M. Zijlema, E. Rogers and J. Groeneweg.
- Booij, N., R.C. Ris, and L.H. Holthuijsen, 1999: A third generation wave model for coastal regions, Part I, Model description and validation. *J. Geophys. Res.*, 104, C4, 7649-7666.
- SWAN team, 2007: SWAN cycle III, version 40.51, Technical documentation. Delft University of Technology.
- Van Dongeren, A.R., J. Groeneweg, G.Ph. van Vledder, A.J. van der Westhuysen, S. Caires and J. Adema, 2007: Hindcasting of waves and wave loads on Dutch Wadden Sea Defenses. Proc. 10th Int. Workshop on Wave Hindcasting and Forecasting, North Shore, Oahu, Hawaii.
- Van der Westhuysen, A.J., M. Zijlema, and J.A. Battjes, 2007: Nonlinear saturation-based whitecapping dissipation in SWAN for deep and shallow water. *Coastal Engineering*, **54**, 151-170.
- WL | Delft Hydraulics, 2007: Reducing the computational time of SWAN by dynamic deactivation of grid points. Report H4918.37, Author: A.J. van der Westhuysen.
- Zijlema, M., A.J. van der Westhuysen, 2005: On convergence behaviour and numerical accuracy in stationary SWAN simulations of nearshore wind wave spectra. *Coastal Engineering*, **52**, 237-256.